Bioactive Materials 6 (2021) 951–962

Contents lists available at ScienceDirect

Bioactive Materials

journal homepage: http://www.keaipublishing.com/biomat

Click CAR-T cell engineering for robustly boosting cell immunotherapy in blood and subcutaneous xenograft tumor

Hong Pan[a,b,1], Wenjun Li[a,1], Ze Chen[a,1], Yingmei Luo[a], Wei He[a], Mengmeng Wang[a], Xiaofan Tang[a], Huamei He[a], Lanlan Liu[a,b], Mingbin Zheng[a], Xin Jiang[a], Ting Yin[a], Ruijing Liang[a], Yifan Ma[a,b,**], Lintao Cai[a,*]

[a] Guangdong Key Laboratory of Nanomedicine, CAS-HK Joint Lab of Biomaterials, CAS Key Lab for Health Informatics, Shenzhen Engineering Laboratory of Nanomedicine and Nanoformulations, Shenzhen Institutes of Advanced Technology (SIAT), Chinese Academy of Sciences, Shenzhen, 518055, PR China
[b] HRYZ Biotech Co., Shenzhen, 518057, PR China

ARTICLE INFO

Keywords:
CAR-T cell
Bioorthogonal click chemistry
Glycometabolic labeling
Off-target effects
Cell immunotherapy

ABSTRACT

The adoptive transfer of chimeric antigen receptor-T (CAR-T) cells has shown remarkable clinical responses in hematologic malignancies. However, unsatisfactory curative results and side effects for tumor treatment are still unsolved problems. Herein we develop a click CAR-T cell engineering strategy via cell glycometabolic labeling for robustly boosting their antitumor effects and safety in vivo. Briefly, paired chemical groups (N_3/BCN) are separately incorporated into CAR-T cell and tumor via nondestructive intrinsic glycometabolism of exogenous Ac_4GalNAz and Ac_4ManNBCN, serving as an artificial ligand-receptor. Functional groups anchored on cell surface strengthen the interaction of CAR-T cell and tumor via bioorthogonal click chemistry, further enhancing specific recognition, migration and selective antitumor effects of CAR-T cells. In vivo, click CAR-T cell completely removes lymphoma cells and minimizes off-target toxicity via selective and efficient bioorthogonal targeting in blood cancer. Surprisingly, compared to unlabeled cells, artificial bioorthogonal targeting significantly promotes the accumulation, deep penetration and homing of CAR-T cells into tumor tissues, ultimately improving its curative effect for solid tumor. Click CAR-T cell engineering robustly boosts selective recognition and antitumor capabilities of CAR T cells in vitro and in vivo, thereby holding a great potential for effective clinical cell immunotherapy with avoiding adverse events in patients.

1. Introduction

T-cells engineered to express Chimeric Antigen Receptors (CARs), so-called 'living drugs', has emerged as a promising approach for cancer immunotherapy, particularly in the treatment of blood cancers [1–3]. However, CAR-T therapy often comes with serious on-target/off-tumor effects from its insufficient immune recognition, such as normal B-cell aplasia and tumor antigen escape [4–7]. Additionally, the immunosuppressive tumor microenvironment as a major obstacle also seriously inhibited the infiltration, accumulation, and survival of CAR-T cells in tumor [8,9]. Thus, the ideal cancer treatment may require a novel armored CAR-T cell, which has been further engineered to boost antitumor efficacy and reduce adverse events.

It was reported that close contact between immune cell and tumor cell is essential for intercellular immune recognition, communication, activation, and final cytotoxicity in the antitumor immune responses [10,11]. Considering that cell-cell interaction in nature is typically achieved by contact-mediated connections of surface adhesion molecules and receptors [12–14], T cells genetically expressed additional tumor antigen adhesion receptor, such as CD20, CD22 and HER2, can effectively resist tumor progression [15,16]. Thus, artificial modification on T cell surface with an additional ligand-receptor might be simple and effective strategy for improving its anti-tumor effects. This approach will also shed a light on strengthening the interaction between CAR-T cell and tumor via introducing efficient and special artificial targets to improve the antitumor effects and reduce unwanted toxicities during cancer therapy.

In recent years, bioorthogonal glycometabolic engineering was

Peer review under responsibility of KeAi Communications Co., Ltd.
* Corresponding author.
** Corresponding author. HRYZ Biotech Co., Shenzhen, 518057, PR China.
E-mail addresses: yf.ma@siat.ac.cn (Y. Ma), lt.cai@siat.ac.cn (L. Cai).
[1] These authors equally contributed to this paper.

https://doi.org/10.1016/j.bioactmat.2020.09.025
Received 12 August 2020; Received in revised form 21 September 2020; Accepted 27 September 2020

developed into a reliable technique for modulating cell-surface carbohydrates by the biosynthetic incorporation of unnatural sugars, which has emerged as a powerful tool to artificially label and modify target cells [17–19]. This novel technology employed the concept of artificial bioorthogonal targeting via chemical reaction between functional chemical reporters and their complementary groups in vivo [20,21]. Azide molecules conjugated monosaccharides are wildly used for glycometabolic labeling of target cells, due to its accessibility, small size, inertness and near absence in living system [22–24]. Additionally, our previous studies also showed the bicycle [6.1.0] nonyne (BCN) motif modified on mannose (Ac_4ManNBCN), a complementary group of azide molecule, exhibited high efficiency for introducing BCN group into tumor cell surface [25,26]. As a result, once the paired chemical reporters (-N_3/-BCN) are introduced to CAR-T and tumor cells separately, bioorthogonal chemistry-guided specific targeting could facilitate connection and activation of CAR-T cell to tumor, thereby further enhancing their antitumor capability.

In this work, a click CAR-T cell engineering strategy was performed for boosting the therapy of CAR-T cells against tumor through metabolic engineering of unnatural sugars containing chemical functional groups. The paired functional groups (-N_3/-BCN) were efficiently and nondestructively incorporated into cell-surface glycans of CAR-T cell and B lymphoma cell tumor via glycometabolic engineering of Ac_4GalNAz and Ac_4ManNBCN, respectively. The azide armored CAR-T (N_3-CAR-T) cell dramatically enhanced the recognition, migration and selective killing for BCN-Raji cell via bioorthogonal chemistry-triggered cell-cell contact. In mice, N_3-CAR-T cells not only obviously enhanced efficacy for removing B-cell lymphoma, decreasing the unwanted toxicity in blood tumor model, but also significantly improved infiltration and homing of CAR-T cells into tumor tissues and further inhibited the growth of solid tumor (Scheme 1). This click CAR-T cell engineering based on cellular complementary bioorthogonal glycometabolic labeling provided a reliable strategy for CAR-T cell therapy with high efficiency and safety, thereby further boosting clinical effects of cell immunotherapy in cancer treatment.

2. Experimental section

2.1. Regents and cell line

K562 and Raji cells with or without firefly luciferase were obtained from Cell Bank Shanghai Institutes Life Sciences under Chinese Academy of Science and cultured as each recommendations. Anti-CD3, anti-CD8 and anti-CD19 monoclonal antibodies were purchased from BD Bioscience. Azido sugar (Ac_4GalNAz), tetrazine conjugated Cy5 (Tz-Cy5) and Dibenzocyclooctyl (DBCO) conjugated Fluor 488 (DBCO-Fluor 488) were purchased from Click Chemistry tools (Scottsdale, AZ, USA). Other chemicals and reagents for BCN-sugar (Ac_4ManNBCN) synthesis were obtained from Aladdin or Sigma-Aldrich.

2.2. Production of CAR-T cells

Human peripheral blood mononuclear cells (PBMCs) were isolated from the heparinized peripheral blood of healthy volunteers by discontinuous density gradient centrifugation. To rapidly obtain human T cells, 5×10^6 isolated PBMCs seed in 25 cm^2 cell culture flask were stimulated with Dynabeads® Human T activator CD3/CD28 (Thermo Fisher) at a bead-to-cell ratio of 1:1 in the AIM-V media preserved 2% FBS (Gibco, BRL Co. Ltd., USA) and 300 IU/mL of human exogenous rIL-2 (PeproTech Inc., USA) for additional 5 days. For producing of the effective CD19 CAR-T cells, the expanded T cells were transduced with lentivirus as our previously described method [24]. Flow cytometry analysis indicated that the percentage of CD19 CAR positive T cells could reach ~75% under indicated preparation conditions.

2.3. Unnatural sugar incorporation and bioorthogonal labeling

The BCN group modified sugar Ac_4ManNBCN was synthesized as our previously described methods [25]. Raji cells were incubated with Ac_4ManNBCN at the different concentrations (10, 15, 20 μM), and cultured for 48 h. The BCN group modified on Raji cells was detected by N_3-Cy5.5 (Click Chemistry Tools, AZ) using a confocal laser scanning microscope (TSC SP5II Leica, Ernst-Leitz-Strasse, Germany). To determine labeling efficiency of BCN groups, cells were re-suspended in PBS containing 0.5% FBS and reacted with N_3-Cy5.5 for 30 min, followed by flow cytometry analysis. To modify the solid tumor, the Raji tumor with intratumoral administration of Ac_4ManNBCN was harvested for confocal imaging and flow cytometry analysis using N_3-Cy5.5 probe.

To incorporation of azide group into CAR-T cell surface, the human PBMCs were pre-treated by anti-CD3/CD28-coated beads and rIL-2 for 3–4 d, and then a serial concentration (25, 50, 100 μM) of azido sugar (Ac_4GalNAz) were added respectively to completed AIM-V media and co-cultured for another for 48 h. To identify the modification of azide group on T cell surface, the confocal imaging and flow cytometry assay were performed as the methods mentioned above using DBCO-Fluor 488 chemical staining.

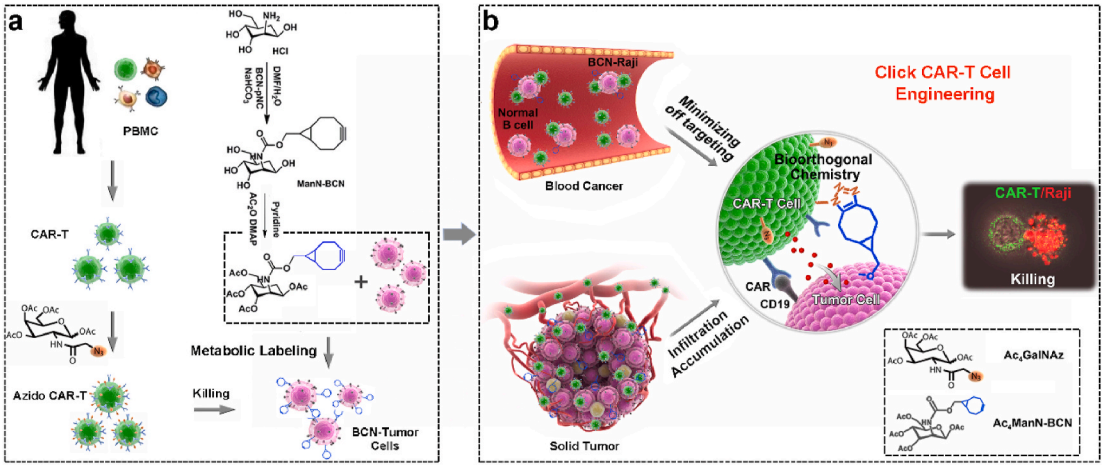

Scheme 1. The scheme of click CAR-T cell engineering for boosting CAR-T cell antitumor efficacy and safety in vivo. (a) CAR-T cells and tumor were labeled with paired functional groups as an additional 'ligand-receptor' by bioorthogonal glycometabolic engineering for facilitating the interaction between CAR-T cell and tumor in blood cancer and solid tumor, respectively. (b) This artificial targeting strategy effectively promoted CAR-T cell selectivity, infiltration and homing to tumor, and thereby dramatically boosting its antitumor capabilities and safety during immunotherapy.

2.4. Cell viability assay

To explore the effects of glycometabolic engineering on the proliferation of tumor and CAR-T cells. The Raji cells were incubated with a serial concentration of Ac_4ManNBCN for 48 h, and cell viability was assessed using Cell Counting Kit-8 (CCK-8) according to manufactory protocol (Dojindo Molecular Technologies, Japan). When the human PBMCs were stimulated by beads and rIL-2 for 3–4 day, the obtained human T cells were incubated with 50 μM of Ac_4GalNAz for another 48 h. After the incubation, the cell viability was also assessed using CCK-8 kit according to previously described method.

2.5. Targeting assays

The targeting of N_3-CAR-T cell to BCN-Raji cell was analyzed using confocal immunofluorescence imaging. CAR-T cells and Raji cells with or without labeling were immunostained with anti-CD3 (APC) or anti-CD19 (PE) antibodies respectively for 30 min at ice. Subsequently, the stained CAR-T cells were seeded into 8-well lab-Tek chamber slides (Thermo Fisher Scientific Inc. Waltham, MA) at ratio of 1:1 with stained Raji cells, and then incubated in a humidified incubator at 37 °C and 5% CO_2 for 10–20 min. The fluorescent images were captured at indicated time points using the confocal laser scanning microscope.

2.6. CAR-T cell migration assay

1×10^6 CAR-T cells with or without azide modification were suspended in serum free RPMI media and loaded in the upper chamber of 5.0 μm pore size transwell apparatus (Corning, Lowell, MA). 5×10^5 Raji cells with or without BCN group in serum free RPMI were added in the basolateral chamber of the transwell. After 4 h of co-culture at 37 °C, the migrated CAR-T cells were harvested from the basolateral chamber and counted by flow cytometry using anti-CD3 and anti-CD19 monoclonal antibody, respectively.

2.7. Cytokine release

Cytokine release assays were performed by overnight co-culture of N_3-CAR-T cells and Raji cells with or without Ac_4ManNBCN administration at the ratio of 1:1. Cell culture supernatants were harvested and then analyzed for IFN-γ, IL-2, and TNF-α using Enzyme Linked Immunosorbent Assay (ELISA) according to the manufacturer's protocols (eBioscience, Santiago, CA, USA).

2.8. Cytotoxicity assay

Cytolysis activity of CAR-T cells against tumor cells was determined using the CytoTox 96 Non-Radioactive Cytotoxicity Assay (Promega, Madison, USA). CAR-T cells were incubated with Raji or K562 tumor cells at a varied ratios from 1:1 to10:1 and the mixture cells were finally maintained a total cell density of 1×10^6/ml. After 4 h post-incubation, the medium supernatants were collected and measured immediately for LDH activities following the manufacturer's instructions. The percentage cytotoxicity was calculated according to the following formula: Cytotoxicity % = 100 × [((CAR-T cell + target cell) – (CAR-T cell alone + target cell alone))/(max target cell lysis − target cells alone)].

2.9. 3D cell spheroids model

Raji or BCN-Raji tumor cells (0.5×10^4 cells/well) were seeded as co-culture in RPMI 1640 media in cell-repellent surface 96-well microplates (Greiner Bio-One) and immediately centrifuged at 180×*g* for 2 min. Three days after seeding, CAR-T cells with or without azide labeling were added to the spheroids at 5×10^4 cells per well for overnight incubation. Spheroids were washed three times with PBS to remove loosely attached CAR-T cells. The infiltration of CAR-T cells in spheroids was also analyzed by confocal inflorescence imaging using anti-CD3 and anti-CD19 antibodies, respectively. Simultaneously, spheroids were dissociated using Accumax (eBiosciences) for 90 min for CAR-T cell quantification by flow cytometry. To determine the cytotoxicity of CAR-T cells in spheroids, the live/apoptosis tumor cells were detected by Calcein-AM/PI staining assay after 24 h of incubation.

2.10. Tumor xenograft models

In brief, 6–8-week-old NOD/SCID mice were bred in house under an approved Institutional Animal Care and Use Committee protocol. To carry out the blood tumor models, NOD/SCID mice were intravenously inoculated with 5×10^5 luciferized Raji cells (day 0). On day 7, 1×10^7 CAR-T cells (~75% CAR^+) with or without azide group modification were infused intravenously as previously described [27]. PBS treated animals served as controls. In the solid tumor model, to obtain the BCN motif modified solid tumors, Raji-Luci tumor cells (1.0×10^7 cells) were subcutaneously inoculated on the dorsal flank of mice. When the tumor reached about 100 mm^2, Ac_4ManNBCN (40 mg/kg) or equal value of PBS were administered into Raji tumor-bearing mice by intratumoral injection once a day for 4 days. Next, a dose of 1×10^7 CAR-T cells (~75% CAR^+) with or without azide modification were infused intravenously every three days.

After intraperitoneal injection of D-Luciferin (150 mg/kg), tumor burden of mouse was measured by the IVIS® system (Caliper) as radiance in the region of interest. Mice were sacrificed upon losing more than 15% of body weight or the development of hind limb paralysis. To reduce the effect of insufficient of ATP and oxygen ex vivo, luciferin signal was detected and quantified in tissue/organ samples using IVIS system in 5–10 min, including the tumor, heart, liver, spleen, lung, kidney and thighbone. To determine Raji cell number in blood, 50 μl of murine blood was drawn at the end of experiments, and the harvested cells were analyzed by flow cytometry using anti-CD19 (PE) antibodies. After tumor digestion by collagenase/DNase, CAR-T cell infiltrated in tumor was analyzed using flow cytometry with anti-CD3, anti-CD8 or *anti*-Myc-alexa 488 antibodies, respectively. Each tumor tissue is obtained from their matched tumor-burden mouse, and all animal samples were participated in the whole experimental process (n = 5).

2.11. Histological staining

For tissue immunostaining, the tumor, heart, liver, spleen, lung and kidney tissues were harvested at 28 d post administration, and embedded in OCT and cut into 8 μm sections, followed by stained with anti-CD3, anti-CD8 or *anti*-Myc tag antibodies respectively. The fluorescent images were recorded by confocal microscopy followed by semi-quantitation using Image-Pro Plus software. To evaluate CAR-T cell infusion-induced pathological change, the above tissues were also stained with hematoxylin and eosin (H&E) according to the manufactory's protocol (Sigma-Aldrich).

2.12. Statistical analysis

Experiment data were expressed as the mean ± standard deviation from at least four independent experiments. The differences among groups were calculated using Student's t-test or one-way ANOVA analysis followed by Tukey' s post-test (GraphPad Prism, GraphPad Software, La Jolla, CA). Differences were considered significant at $^*p < 0.05$, $^{**}p < 0.01$, and $^{***}p < 0.001$.

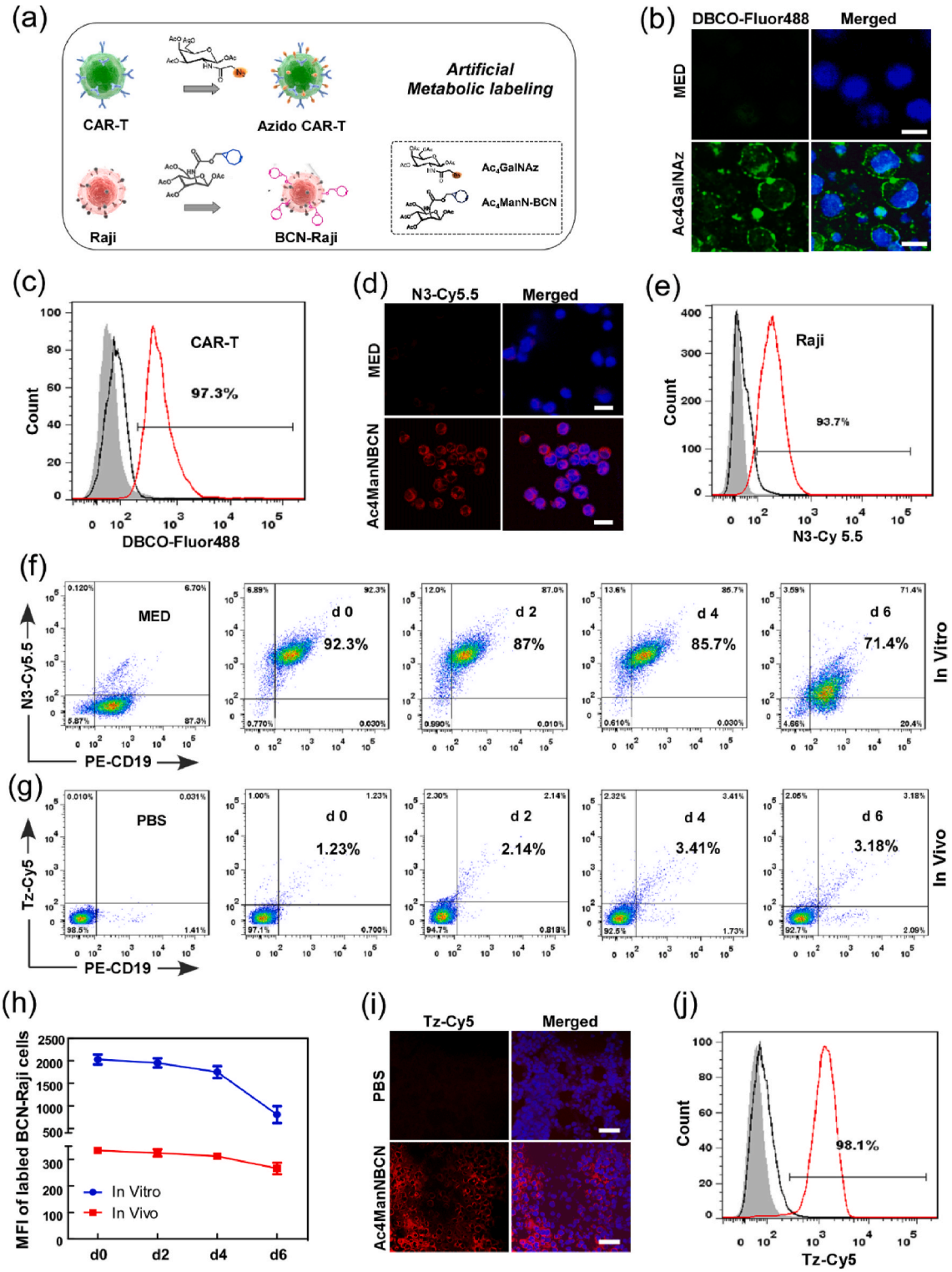

Fig. 1. The glycometabolic labeling performance of azido-or BCN-sugar in active CAR-T and tumor cells, respectively. (a) The scheme of artificial metabolic labeling for CAR-T and tumor cells. (b–e) Confocal imaging and flow cytometry analyses of CAR-T and Raji cells separately stained with DBCO-Fluor488 and N_3-Cy5.5 for 30 min after incubation with Ac_4GalNAz and Ac_4ManNBCN, respectively. Scale bar = 10 μm. (f–h) Flow cytometry analyses of the stability of BCN group on Raji cell in vitro and in vivo from day 0 to day 6 post labeling of BCN groups using Ac_4ManNBCN. (i–j) The generation of BCN groups on tumor tissues were analyzed by confocal microscopy and flow cytometry using Tz-Cy5 probe. Scale bar = 20 μm.

3. Results

3.1. Efficient cellular glycometabolic modification for CAR-T and tumor cells

To modify the functional chemical groups on CAR-T cells and Raji tumor cells, both the cells were treated with N_3- or BCN-sugar respectively for 48 h (Fig. 1a). Cell-surface –N_3 and -BCN groups were separately detected by DBCO- or azide-terminated fluorophore (DBCO-Fluor488 and N_3-Cy5.5), and then analyzed by confocal imaging and flow cytometry. Unnatural sugar, especially Ac_4GalNAz, treated CAR-T cells exhibited robust fluorescence labeling in a dose-dependent manner, indicating the efficient metabolic incorporation of bio-functional unnatural sugar into CAR-T cells (Fig. 1b–c and **S1a**). As shown in Fig. 1**d-e**, Raji cells treated with Ac_4ManNBCN displayed strong Cy5.5 fluorescence intensity on the cell surface, indicating the successful expression of BCN groups. In addition, we evaluated the effect of unnatural sugar administration on cell viability using CCK-8 assay. As the results, the administration of Ac_4GalNAz (50 μM) and Ac_4ManNBCN (20 μM) had no effects on CAR-T or tumor cell proliferation, respectively (Figs. S1b and S2), suggesting a good bio-safety of cell glycometabolism. To further determine the stability of BCN groups on Raji cell, we also tested the expression level of BCN groups on BCN-Raji cell in medium without BCN-sugar or blood tumor model from day 0 to day 6. The flow data demonstrated that Raji cells maintained stronger Cy5.5 fluorescence intensity from day 0 to day 4, and it decreased to some extent until on day 6 both in vitro and in vivo (Fig. 1f–h), suggesting metabolism modification of BCN-sugar has a better stability on Raji tumor cells.

Simultaneously, we also analyzed metabolic labeling of BCN-sugar in solid Raji tumor tissues by intratumorally administrated with Ac_4ManNBCN. The confocal imaging in tumor tissues showed that almost all tumor tissues treated with Ac_4ManNBCN were labeled by tetrazine-conjugated fluorescence probes (Tz-Cy5) via bioorthogonal chemistry. In contrast, there was no significant fluorescent signals were observed in the control groups (Fig. 1i). Moreover, the labeling efficiency of tissues with fluorophore Cy5 was analyzed by flow cytometry. The flow cytometry data showed that 98.1% of Cy5-positive cells were detected in the tumor tissue with BCN-sugar administration (Fig. 1j), remarkably consistent with the results of tissue fluorescence imaging. These data suggested that BCN-sugar were able to effectively metabolic labeled Raji solid tumors with BCN groups in vivo, which will provide an artificial bioorthogonal targeting for anti-tumor treatment in the follow-up experiments.

3.2. Artificial bioorthogonal targeting enhances the interaction of CAR-T cells for B lymphoma cells

Although CAR-T cells can effectively recognize tumor through the special bind between CAR and targeting antigen, some tumor cells can escape killing via antigen escape triggered by spontaneous mutation and selective expansion of antigen-negative tumor cells [28–30]. To enhance tumor targeting capacity, CAR-T cells administered with Ac_4GlcNAz (N_3-CAR-T) were incubated with Ac_4ManNBCN-treated Raji cells (BCN-Raji), and the recognition of CAR-T cell to Raji cell was analyzed by confocal imaging. The fluorescent images showed that the number of cluster of N_3-CAR-T cells and BCN-Raji cells was 2-fold of that of CAR-T cell and Raji cells at 20 min (Fig. 2a–b), indicating click functional groups on cell surface enhanced the recognition of CAR-T cell to Raji cell. Moreover, compared to the cells without metabolic labeling, N_3-CAR-T cells can rapidly bind BCN-Raji cells and aggregated into bigger cell clusters from 0 to 20 min. To further confirm the interaction of N_3-CAR-T cell and BCN-Raji cell, in vitro cell migration and invasion were also performed using transwell chambers and flow cytometry assay. The results clearly revealed that artificial targeting strategy increased the invasion of CAR-T cells by 20% compared with unlabeled controls (Fig. 2c).

For mechanistic in vitro studies on the role of bioorthogonal targeting in CAR- T cell infiltration within tumor, lymphoma spheroids of Raji cells were established using three-dimension (3D) cell culture system as previous studies [31,32]. As we expected, bioorthogonal modification effectively enhanced the infiltration depth of CAR-T cells into Raji spheroids in a relatively short time (Fig. 2d). Flow cytometry analysis also showed the number of CAR-T cells in the spheroids was also obviously increased by artificial bioorthogonal targeting (Fig. 2e–f). Next, we further assessed the capacity of antitumor cytokine production of the CAR-T cells as indicated above conditions. As shown in Fig. 2g–i, click CAR-T cells significantly increased the expression of cytokine IL-2, IFN-γ and TNF-α when compared to CAR-T cells alone, indicating artificial targeting boosting anti-tumor cytokine secretion of CAR-T cells. Taken together, these data distinctly demonstrated that not only artificial bioorthogonal targeting rapidly increased the recognition and adhesion of CAR-T cell to B lymphoma Raji cell, but also enhanced the migration, infiltration and anti-tumor response of CAR-T cells in vitro.

3.3. Artificial bioorthogonal targeting selectively boosts CAR-T cell antitumor capability

The interaction between CAR-T cells and tumor cells also detailed investigated by measuring killing activity of CAR-T cells against Raji cells. The distinct dynamic profiles of tumor killing by CAR T cells were examined and analyzed using live fluorescence imaging and flow cytometry assay, respectively. Compared to unlabeled cells, Raji cells were quickly stained by PI and more PI-positive cells were observed in BCN/N_3-labeled group from 1 to 3 h (Fig. 3a–b), indicating more effective tumor killing after incubation with modified CAR-T cells. Simultaneously, bioluminescence imaging assay and Calcein-AM/PI staining also proved the excellent cytotoxicity efficacy of N_3-CAR-T cells against BCN-Raji cells compared to the unlabeled cell group (Fig. S3 and Fig. S4), further confirming the action of artificial bioorthogonal targeting for enhancing CAR-T cell cytotoxicity.

To further explore the mechanism of bioorthogonal modification in enhanced anti-tumor immunity, CAR-T cells were separately incubated with Raji cells or $CD19^{neg}$ K562 cells under the condition with or without bioorthogonal targeting, and then the lactose dehydrogenase (LDH) activity was measured. The results showed that unlabeled CAR-T cells was ~65% killing efficiency in Raji cells, and N_3-CAR-T cells exhibited stronger cytotoxic effect on BCN-Raji cells (~93%) (Fig. 3c). Interestingly, we also clearly found that bioorthogonal modification could effectively enhance the recognition and adhesion of CAR-T and $CD19^{neg}$ K562 cells (Fig. S5), but it did not significantly improve killing efficiency of CAR-T cell against $CD19^{neg}$ K562 as Raji cell (Fig. S6), probably due to lack of special CD19 antigen on K562 tumor cells. More importantly, compared to the unlabeled CAR-T cells, azido CAR-T cells significantly boosted their cytotoxicity to BCN-Raji cells in the mixture of Raji and BCN-Raji cell (Fig. 3d–e). These data suggested that artificial bioorthogonal targeting selectively and effectively boosted the cytotoxicity of CAR-T cells against Raji cells, which was depended on the recognition and interaction between CAR-T cells and its special tumor cells. In addition, the effect of bioorthogonal targeting on CAR-T cytotoxicity was also evaluated in vitro tumor model, the killing of CAR-T cell against tumor spheroids were analyzed using Calcein AM/PI staining. The fluorescent images and flow cytometry analysis showed more apoptotic tumor cells was detected in bioorthogonal group than unlabeled controls (Fig. 3f–h), which can be attributed to bioorthogonal targeting-boosted CAR-T cell infiltration in tumor spheroids as previously mentioned (Fig. 2d–e).

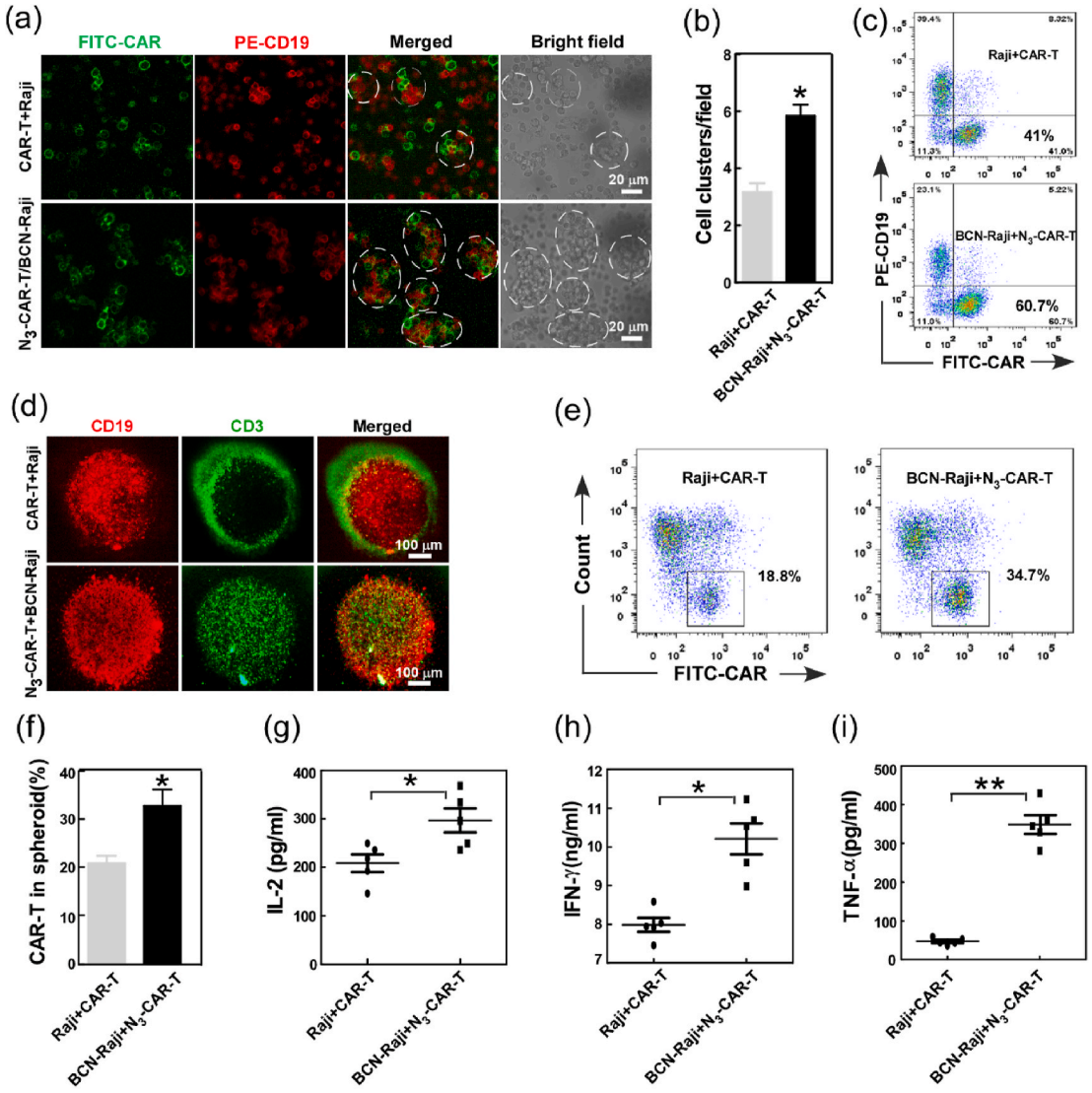

Fig. 2. The effect of artificial bioorthogonal targeting over cell surface on CAR-T cell recognition, migration, and antitumor response. (a) The interaction between CAR-T and Raji cell was analyzed by confocal imaging. The white circles indicated cell clusters of T and Raji cells. (b) the number of cell cluster in the co-culture of CAR-T and Raji cells with or without treatment by Ac_4ManN-BCN (20 μM) and $Ac_4GalNAz$ (50 μM) respectively, at early 20 min. (c) Transwell assay of CAR-T cell migration with or without bioorthogonal targeting using flow cytometry. (d) Fluorescence imaging analysis of CAR-T cell infiltration into tumor spheroids.(e-f)CAR-T cell infiltration was quantified by flow cytometry using *anti*-Myc tag antibodies. (g–i) The release of IL-2, IFN-γ and TNF-α was determined using ELISA assay. $^*p < 0.05$, $^{**}p < 0.01$.

3.4. Click CAR-T cell safely and efficiently removes B-cell lymphoma in vivo via artificial bioorthogonal targeting

The effects of artificial bioorthogonal targeting on CAR-T cell anti-tumor capability were further determined in blood tumor mice model. 6-8 week-old NOD/SCID mice were intravenously (i.v.) inoculated with Raji-Luci cells with or without $Ac_4ManNBCN$ administration, followed by i. v. injection by N_3-CAR-T or unlabeled CAR-T cells on day 6 after tumor inoculation, respectively (Fig. 4a). For comparing with therapeutic effect, some tumor-bearing mice were i. v. injection with phosphate buffered saline (PBS) as negative control. The bioluminescence imaging showed that mice administrated with N_3-CAR-T cells exhibited extremely weak signal from day 15 to day 28 when compared to unlabeled CAR-T cell treated mice. However, the mice treated with PBS showed stronger bioluminescence signal on the early time of day 10 and the signal intensity reached peak on day 20 (Fig. 4b–c), suggesting artificial bioorthogonal targeting significantly enhanced the efficiency of CAR-T cell for killing Raji cells in vivo. To make a more comprehensive evaluation for therapeutic effect of CAR-T cells, the body weight and survival rate of mice were also separately measured and monitored during animal experiments. The body-weight of mice with bioorthogonal targeting treatment kept steady from d 5 to d 28, while the mice with unlabeled CAR-T cell administration appeared significant weight loss at d 28, especially the body-weight of control mice decreased by 17% from d 5 to d 20 (Fig. 4d). After the final trial, all mice in the PBS control and 3 of 7 mice in unlabeled CAR-T cell treated groups died by day 32 after tumor inoculation. In contrast, mice treated with N_3-CAR-T cells showed markedly increased survival (Fig. 4e). These data suggested that the CAR-T cell therapy based on bioorthogonal targeting significantly remove tumor cells and improve the survival of tumor-bearing mice.

The effect of bioorthogonal targeting on CAR-T cell mediated tumor cell clearance was further evaluated by tissue bioluminescence imaging and flow cytometry analysis. Ex vivo bioluminescence imaging showed that the controls exhibited strong bioluminescent signal in lung and thigh bones, indicating untreated Raji-Luci cells mainly located in this two tissues of mice. However, compared to unlabeled CAR-T cell, CAR-T cells with bioorthogonal targeting resulted in extremely weak signal

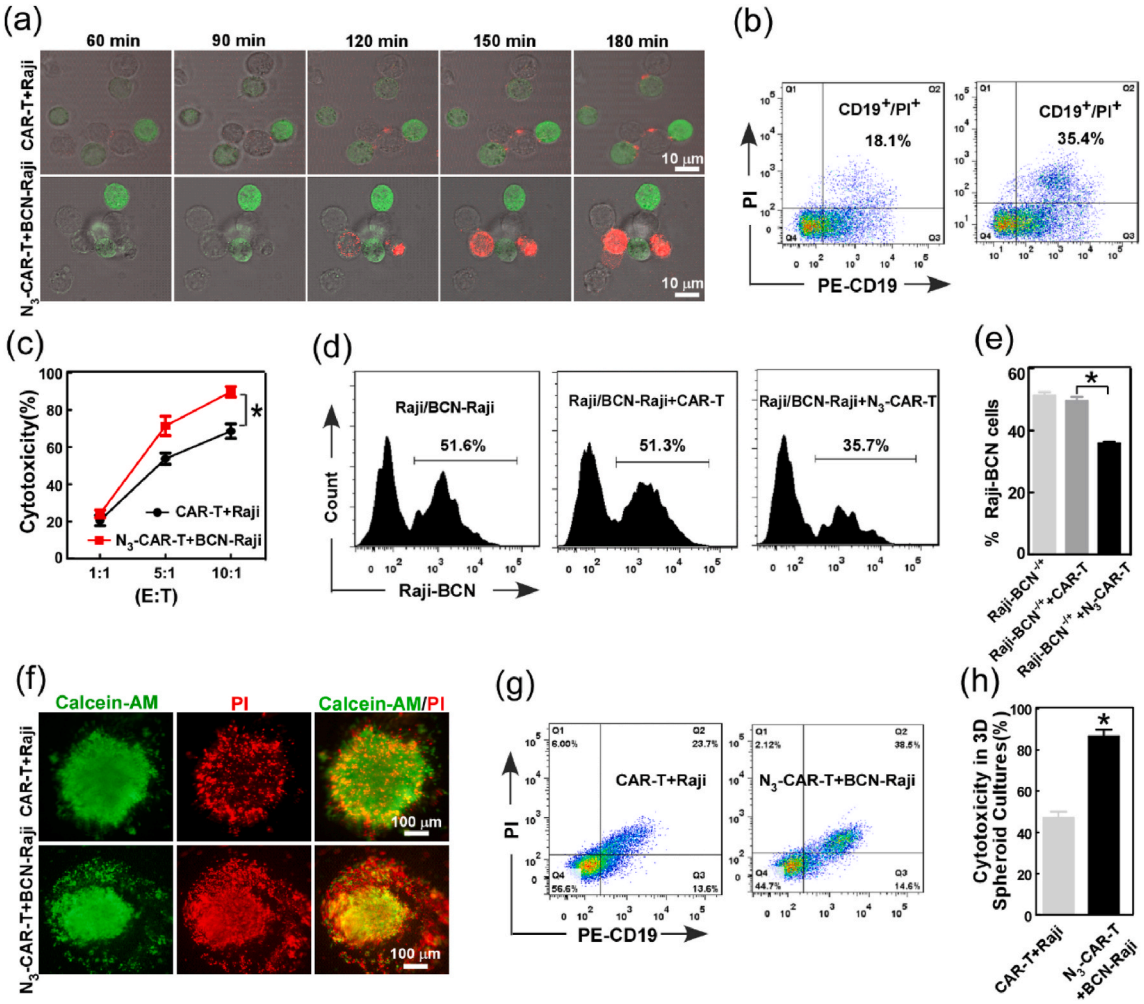

Fig. 3. Bioorthogonal targeting selectively and effectively boosted cytotoxicity of CAR-T for tumor cells. (a) Time-lapse live microscopy was used to measure CAR-T cell cytotoxicity against target cells in the presence of PI (100 μM). Images were acquired every 30 min, and displayed the overlays of the anti-CD3-FITC antibody (green), PI (red), and bright field channels.(b) The apoptosis of Raji cells were analyzed by flow cytometry using PI at 3 h post administration of CAR-T cells. (c) LDH release analysis of CAR-T cell killing activity to Raji cells. (d–e) Flow cytometry analysis evaluated the selective cytotoxicity of azido CAR-T cells in mixed Raji cells. (f-h) The killing activity of CAR T cells with or without bioorthogonal targeting was analyzed using the 3D tumor spheroid model. The death rate of tumor cells in 3D tumor spheroids was separately analyzed using confocal imaging and flow cytometry at 24 h post-incubation.

in lung and thigh bone tissue of tumor-bearing mice (Fig. 4f–g). Simultaneously, peripheral blood of mice was harvested and the percentage of Raji-Luci cells in blood was quantified using flow cytometry on day 28 after tumor inoculation. As shown in Fig. 4h–i, the percentage of Raji-Luci cells in blood of bioorthogonal targeting group decreased by nearly 10-folds when compared to unlabeled CAR-T cell treated mice. In contrast, the percentage of Raji-Luci cell in blood of control group increased up to 10.1%. These data clearly demonstrated that CAR-T cells with bioorthogonal targeting rather than unlabeled cells could completely eliminate tumor in mice.

It is also important to increase the safety of CAR-T cell therapy when improving the specificity of the modified T cells [33,34]. To assess the potential toxicity of CAR T cell therapy, susceptible murine organs, including the heart, liver, spleen, lung, and kidney, were excised and examined histologically. No off-target toxicity was detected against these indicated organs after injection of N_3-CAR T cells. However, unlabeled CAR-T cell administration caused serve pathological lesions in different organs, such as inflammatory cell infiltration and significant epithelium thickening in the alveoli (Fig. S7). More importantly, there are no obvious infiltration of extraneous CAR-T cell was observed in lung and spleen tissue of azido CAR-T cell group compared to CAR-T cell treated mice alone (Fig. S8), indicating the extra bioorthogonal targeting modification could effectively avoid CAR-T cell cytotoxicity to normal cells. Hence, the CD19 specific CAR-T cell therapy based on artificial bioorthogonal targeting was safe and had no off-target toxicity on mice.

3.5. *Click CAR-T cell effectively delays the growth of subcutaneous xenograft tumor via artificial bioorthogonal targeting*

In consideration of excellent therapeutic effect of CAR-T cells with bioorthogonal targeting in blood cancer, thus the potency of this targeting strategy was also investigated in solid tumor model. Raji cell not only is well known blood cancer model due to CD19 molecule targeting, but also can grow into tumor tissues in mouse subcutaneous like other solid tumor cells. Thus, the Raji cell subcutaneous xenograft model was adopted to study the targeting and antitumor effect of click CAR-T cell. CAR-T or N_3-CAR-T cells were intravenously injected into tumor-bearing mice which were pretreated with either PBS or Ac_4ManNBCN, respectively (Fig. 5a). Next, the burden of tumor in mice were analyzed by time-dependent in vivo and ex vivo bioluminescence imaging analysis. The signal intensity in tumor of mice in PBS control was about 1.8-fold higher than CAR-T cell group, and 10-fold higher than experimental group with bioorthogonal targeting on the day 25 post CAR-

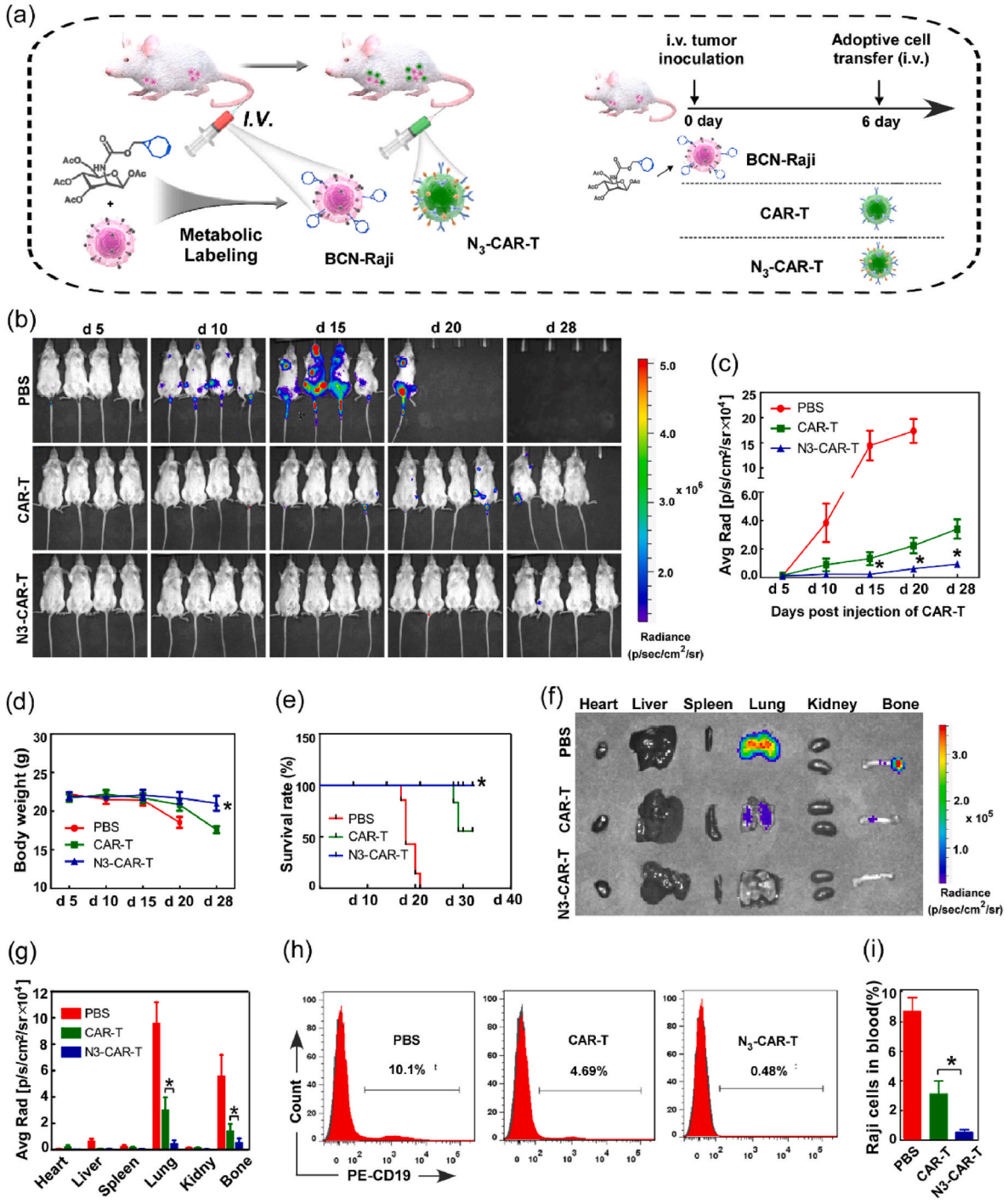

Fig. 4. The artificial bioorthogonal targeting effectively boosted tumor clearance by CAR-T cells in blood cancer. (a) Raji-luci cells with or without BCN-motifs were intravenously inoculated into 6-week-old NOD/SCID mice. Six days later, mice were infused intravenously with indicated CAR-T cell every other week. (b) Tumor burden was monitored by bioluminescence imaging (BLI) every few days, and (c) quantified by the radiance detected in the region of interest (ROI). (d) The body weight change and (e) survival rate of mice in each group were separately monitored daily until day 40 post-inoculation. (f) On day 28, mouse organs, including heart, liver, spleen, lung, kidney, and thigh bone, were harvested and imaged by BLI, and (g) quantified by the radiance detected in the ROI. (h–i) The blood of mouse were harvest and the amount of peripheral Raji cells was measured by flow cytometry using anti-human CD19 antibodies. *$p < 0.05$.

T cell injection (Fig. 5b–c). Moreover, the mice were sacrificed and the bioluminescence signal of different organs and tumor were measured at the experimental end. Similarly, the signal intensity of tumor in N_3-CAR-T cell treated mice decreased by 65% than unlabeled CAR-T cell group, but no obvious signal was detected in other organs (Fig. S9). Compared to PBS or unlabeled CAR-T cell treated groups, N_3-CAR T cells led to a dramatic reduction in tumor burden in BCN-modified mice. Next, we also measured the tumor volume and survival of mice from 0 to 32 days post CAR-T cell injection. We found that intravenous delivery of N_3-CAR T cell not only delayed tumor growth, but also was associated with a notably better survival (Fig. 5d–e). In contrast, mice treated with unlabeled CAR-T cells reached a humane experimental end point by 35 days after initial tumor modeling.

Since the efficacy of CAR-T cells is known to be directly proportional to the density and persistence of CAR-T cell in tumor [35–37], the accumulation and infiltration of extraneous T cells in tumor was

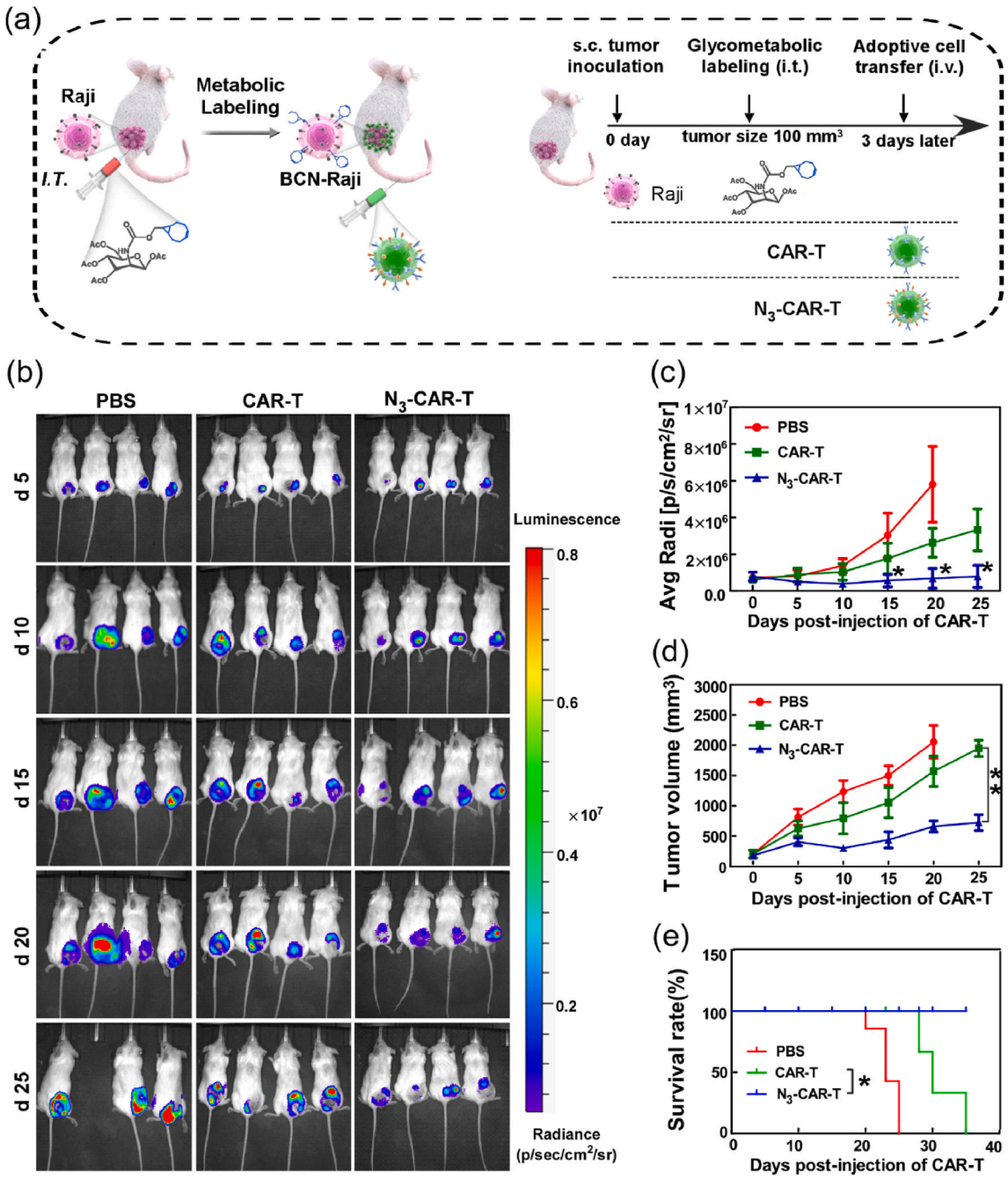

Fig. 5. The antitumor effects of CAR-T cells with metabolic bioorthogonal targeting in solid tumor. (a) NOD/SCID mice bearing Raji-luci tumors with or without Ac_4ManNBCN treatment were treated with an intravenous infusion of 10×10^6 N_3-CAR-T cells or CAR-T cells as previous methods. (b) Tumor burden was monitored by BLI every few days, and (c) quantified by the radiance detected in the ROI. (d) The tumor volume and (e) survival rate of mice in each group were separately monitored daily until day 35 post-inoculation. Data shown are mean ± SEM (n = 5), differences between groups were analyzed using Student's t-test. $^*p < 0.05$, $^{**}p < 0.01$.

further analyzed using quantitative flow cytometry and immunofluorescence assay at experimental end. Our data showed that the number of infiltrated CD3 T and CD8/CAR-T cells in tumor tissue of N_3-CAR-T cell administrated mice was respectively about 2-folds and 2.6-folds higher than that in unlabeled CAR-T group (Fig. 6a–d). It indicated that there were more extraneous CAR T cells without azide tag lose trafficking into tumor during the treatment process. Simultaneously, the tissue immunofluorescence also showed the infiltrated extraneous CD8 T cell in tumor were about 2.5-folds in N_3-CAR-T cell infused mice when compared to unlabeled CAR-T group (Fig. 6e–f), consistent with the previous results of flow cytometry analysis. Surprisingly, the confocal images demonstrated a great many N_3-CAR-T cells trafficked into deep regions of the tumor with sugar treatment, however, most unlabeled CAR-T cells only located tumor tissue edge in the unlabeled group (Fig. 6g). These data suggested that artificial bioorthogonal targeting dramatically boosted the homing and accumulation of extraneous CAR-T cells, particularly the successful trafficking and infiltration of cytotoxic CD8 CAR-T cells in deep tumor tissue, which was crucial for effectively eliminating solid tumor [38,39].

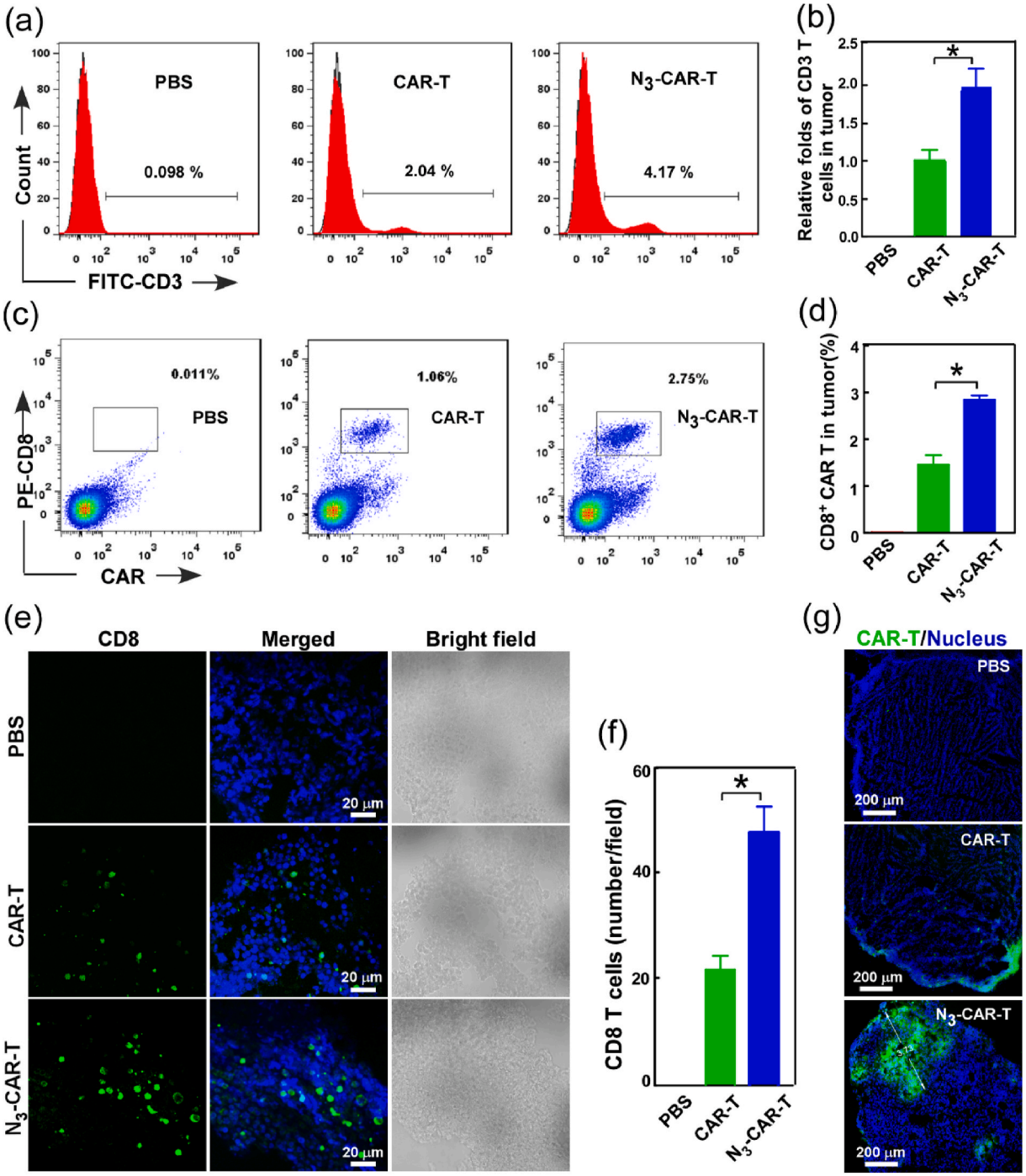

Fig. 6. CAR-T cell penetration and accumulation in Raji solid tumors. NOD/SCID mice bearing Raji tumors with or without Ac_4ManNBCN treatment were administrated by an intravenous injection of 10×10^6 N_3-CAR-T cells or CAR-T cells as previous methods, the tumor tissues have been harvested for the following analysis at 28 d post administration. (a–d) The amount of CAR-T cells in tumor tissues was measured by quantitative flow cytometry analysis using *anti*-Myc tag, anti-CD8 and anti-CD3 antibodies staining, respectively. (e–g) Confocal fluorescent imaging analysis of CAR-T cell penetration and accumulation in distinct regions of tumor tissues using anti-CD8 and *anti*-Myc tag antibodies, respectively. $^*p < 0.05$.

4. Discussion

Given the adverse events and major bottleneck of CAR-T cell therapy, previous many methods has been developed to improve their safety and efficacy. However, these studies on CAR-T cell therapy have been mainly limited in T cell modification and reconstruction in genetic level, including expression functional cytokine/chemokine and active molecules [40,41]. However, these techniques are complex and time-consuming processes, particularly, the curative effect and safety issue remain the major challenge during engineered T cell therapy [42,43]. Herein, we present a novel chemically armored CAR-T cell via introducing artificial bioorthogonal targeting to improve their antitumor effects and reduce unwanted toxicities. The artificial click CAR-T cell engineering not only effectively elevated CAR-T cell recognition, infiltration and homing to tumor tissues, but also significantly enhanced their antitumor efficacy and biosafety in vivo.

Bioorthogonal chemistry based glycometabolic labeling is a novel strategy to achieve cell-cell connection and communication by cell

natural metabolic process. In our study, the paired functional groups were successfully and efficiently incorporated into CAR-T cells and tumor cells with no effects on cell proliferation and functional activities. Particularly, these chemical groups expressed on cell surface can stable in mice for 6 days (Fig. 1), which provided enough time for armored CAR-T cells selectively capturing tumor cells in vivo. We also found that artificial bioorthogonal labeling significantly increased cytokine production, tumor infiltration and cytotoxicity of CAR-T cells, when compared unlabeled CAR-T cell did (Fig. 3). More importantly, the LDH assay showed that CAR-T cells exhibited stronger cytotoxicity against $CD19^+$ Raji cells than $CD19^-$ K562 cells on the same condition of bioorthogonal targeting (Fig. S6). These findings suggested that this cell-cell connection medicated by artificial bioorthogonal targeting could promoted the interaction of CAR-T and tumor cells, thereby further strengthen the CAR-T-cell activation and anti-tumor capability.

Considering CD19 expressed on the surface of B-cell lymphoma and most normal B cells simultaneously, and the off-tumor toxicity related to CAR T-cell therapy is still concerning. Our current study showed that bioorthogonal targeting effectively boosted the specific recognition, infiltration and accumulation of CAR-T cells in different tumor models (Figs. 2, **3** and **6**). Furthermore, we also found that N_3-CAR-T cells can selectively and priorly kill the BCN-Raji cells in the mixture of Raji cells with or without BCN-modification (Fig. 3), which could reduce the potential off-target effect of CAR-T cell therapy. That could be attributed that bioorthogonal targeting triggered high affinity of scFv to CD19 and selectively boosted efficient damage of CAR-T against tumor cells. For safety, we histopathologically examined the potential systemic toxicity in different murine organs and found that bioorthogonal targeting-guided CAR T therapy did not cause notable pathological changes and exogenous T lymphocyte infiltration in major murine organs (Figs. S7 and S8). It clearly demonstrated that artificial bioorthogonal targeting guided CAR-T cell therapy was safe and had no unexpected off-target effects on mice.

5. Conclusion

In conclusion, the present study reported a click CAR-T cell engineering strategy using metabolic bioorthogonal chemistry for boosting the cytotoxicity of CAR-T cells in vitro and in vivo. The artificial bioorthogonal strategy effectively facilitated the interaction between CAR-T cells and tumor, and remarkably elevated antitumor cytotoxicity of CAR-T cells in blood cancer with reducing potential off-target effects. More importantly, this artificial targeting strategy significantly enhanced CAR-T cell accumulation and penetration into deep tumor tissues, and obviously improved the curative effect of solid tumor. Hence, bioorthogonal chemistry-armored artificial modification is an efficient and versatile strategy to boost target recognition and therapeutic efficacy of CAR T cells in vivo, thereby holding a great potential for effective clinical CAR-T and TCR-T cell therapy with avoiding adverse events in patients.

CRediT authorship contribution statement

Hong Pan: conceived the study work, planned the research, The manuscript was written by Hong Pan with substantial help from all other authors. **Wenjun Li:** He planned the research. **Ze Chen:** planned the research. **Yingmei Luo:** planned the research. **Wei He:** planned the research. **Mengmeng Wang:** did the experiments including material synthesis, cell culture, cell labeling and cytotoxicity assay. **Xiaofan Tang:** carried out the animal experiments. Results and data were discussed by. **Huamei He:** did the experiments including material synthesis, cell culture, cell labeling and cytotoxicity assay. **Lanlan Liu:** did the experiments including material synthesis, cell culture, cell labeling and cytotoxicity assay. **Mingbin Zheng:** did the experiments including material synthesis, cell culture, cell labeling and cytotoxicity assay. **Xin Jiang:** carried out the animal experiments. Results and data were discussed by. **Ting Yin:** carried out the animal experiments. Results and data were discussed by. **Ruijing Liang:** carried out the animal experiments. Results and data were discussed by. **Yifan Ma:** conceived the study work, planned the research, The manuscript was written by Hong Pan with substantial help from all other authors. **Lintao Cai:** conceived the study work, The manuscript was written by Hong Pan with substantial help from all other authors.

Declaration of competing interest

The authors declare that they have no known competing financial interests or personal relationships that could have appeared to influence the work reported in this paper.

Acknowledgements

We gratefully acknowledge funding support from the National Natural Science Foundation of China (Grant No. 81971749, 81601552, 31571013), Guangdong Natural Science Foundation of Research Team (2016A030312006), Shenzhen Science and Technology Program (JCYJ20170818163739458, JCYJ20170306160217433, CYZZ20170331150956189).

Appendix A. Supplementary data

Supplementary data to this article can be found online at https://doi.org/10.1016/j.bioactmat.2020.09.025.

References

[1] P.L. Zinzani, Traditional treatment approaches in B-cell non-Hodgkin's lymphoma, Leuk, Lymphoma 44 (Suppl 4) (2003) S6–S14.
[2] C.H. June, R.S. O'Connor, O.U. Kawalekar, S. Ghassemi, M.C. Milone, CAR T cell immunotherapy for human cancer, Science 359 (6382) (2018) 1361–1365.
[3] D.L. Porter, B.L. Levine, M. Kalos, A. Bagg, C.H. June, Chimeric antigen receptor-modified T cells in chronic lymphoid leukemia, N. Engl. J. Med. 365 (8) (2011) 725–733.
[4] E. Zah, M.Y. Lin, A. Silva-Benedict, M.C. Jensen, Y.Y. Chen, T cells expressing CD19/CD20 bispecific chimeric antigen receptors prevent antigen escape by malignant B cells, Cancer Immunol. Res. 4 (6) (2016) 498–508.
[5] M. Hamieh, A. Dobrin, A. Cabriolu, S.J.C. van der Stegen, T. Giavridis, J. Mansilla-Soto, J. Eyquem, Z. Zhao, B.M. Whitlock, M.M. Miele, Z. Li, K.M. Cunanan, M. Huse, R.C. Hendrickson, X. Wang, I. Riviere, M. Sadelain, CAR T cell trogocytosis and cooperative killing regulate tumour antigen escape, Nature 568 (7750) (2019) 112–116.
[6] W.A. Lim, C.H. June, The principles of engineering immune cells to treat cancer, Cell 168 (4) (2017) 724–740.
[7] R.G. Majzner, C.L. Mackall, Tumor antigen escape from CAR T-cell therapy, Canc. Discov. 8 (10) (2018) 1219–1226.
[8] K.G. Anderson, I.M. Stromnes, P.D. Greenberg, Obstacles posed by the tumor microenvironment to T cell activity: a case for synergistic therapies, Canc. Cell 31 (3) (2017) 311–325.
[9] M. Binnewies, E.W. Roberts, K. Kersten, V. Chan, D.F. Fearon, M. Merad, L.M. Coussens, D.I. Gabrilovich, S. Ostrand-Rosenberg, C.C. Hedrick, R.H. Vonderheide, M.J. Pittet, R.K. Jain, W. Zou, T.K. Howcroft, E.C. Woodhouse, R.A. Weinberg, M.F. Krummel, Understanding the tumor immune microenvironment (TIME) for effective therapy, Nat. Med. 24 (5) (2018) 541–550.
[10] K.S.S. Enfield, S.D. Martin, E.A. Marshall, S.H.Y. Kung, P. Gallagher, K. Milne, Z. Chen, B.H. Nelson, S. Lam, J.C. English, C.E. MacAulay, W.L. Lam, M. Guillaud, Hyperspectral cell sociology reveals spatial tumor-immune cell interactions associated with lung cancer recurrence, J. Immunother. Cancer 7 (1) (2019) 13.
[11] G.L. Beatty, W.L. Gladney, Immune escape mechanisms as a guide for cancer immunotherapy, Clin. Canc. Res. 21 (4) (2015) 687–692.
[12] H. Koo, M. Choi, E. Kim, S.K. Hahn, R. Weissleder, S.H. Yun, Bioorthogonal click chemistry-based synthetic cell glue, Small 11 (48) (2015) 6458–6466.
[13] P. Rorth, Communication by touch: role of cellular extensions in complex animals, Cell 112 (5) (2003) 595–598.
[14] D. Kummer, K. Ebnet, Junctional adhesion molecules (JAMs): the JAM-integrin connection, Cells 7 (4) (2018) 25.
[15] T.J. Fry, N.N. Shah, R.J. Orentas, M. Stetler-Stevenson, C.M. Yuan, S. Ramakrishna, P. Wolters, S. Martin, C. Delbrook, B. Yates, H. Shalabi, T.J. Fountaine, J.F. Shern, R.G. Majzner, D.F. Stroncek, M. Sabatino, Y. Feng, D.S. Dimitrov, L. Zhang, S. Nguyen, H. Qin, B. Dropulic, D.W. Lee, C.L. Mackall, CD22-targeted CAR T cells induce remission in B-ALL that is naive or resistant to CD19-targeted CAR immunotherapy, Nat. Med. 24 (1) (2018) 20–28.
[16] C.Y. Slaney, B. von Scheidt, A.J. Davenport, P.A. Beavis, J.A. Westwood,

S. Mardiana, D.C. Tscharke, S. Ellis, H.M. Prince, J.A. Trapani, R.W. Johnstone, M.J. Smyth, M.W. Teng, A. Ali, Z. Yu, S.A. Rosenberg, N.P. Restifo, P. Neeson, P.K. Darcy, M.H. Kershaw, Dual-specific chimeric antigen receptor T cells and an indirect vaccine eradicate a variety of large solid tumors in an immunocompetent, self-antigen setting, Clin. Canc. Res. 23 (10) (2017) 2478–2490.

[17] R.D. Row, H.W. Shih, A.T. Alexander, R.A. Mehl, J.A. Prescher, Cyclopropenones for metabolic targeting and sequential bioorthogonal labeling, J. Am. Chem. Soc. 139 (21) (2017) 7370–7375.

[18] P. Agarwal, B.J. Beahm, P. Shieh, C.R. Bertozzi, Systemic fluorescence imaging of zebrafish glycans with bioorthogonal chemistry, Angew. Chem., Int. Ed. Engl. 54 (39) (2015) 11504–11510.

[19] S.T. Laughlin, N.J. Agard, J.M. Baskin, I.S. Carrico, P.V. Chang, A.S. Ganguli, M.J. Hangauer, A. Lo, J.A. Prescher, C.R. Bertozzi, Metabolic labeling of glycans with azido sugars for visualization and glycoproteomics, Methods Enzymol. 415 (2006) 230–250.

[20] H. Pan, X. Yao, W. Chen, F. Wang, H. He, L. Liu, Y. He, J. Chen, P. Jiang, R. Zhang, Y. Ma, L. Cai, Dissecting complicated viral spreading of enterovirus 71 using in situ bioorthogonal fluorescent labeling, Biomaterials 181 (2018) 199–209.

[21] H. Pan, W.J. Li, X.J. Yao, Y.Y. Wu, L.L. Liu, H.M. He, R.L. Zhang, Y.F. Ma, L.T. Cai, In situ bioorthogonal metabolic labeling for fluorescence imaging of virus infection in vivo, Small 13 (17) (2017) 1604036.

[22] B.R. Varga, M. Kallay, K. Hegyi, S. Beni, P. Kele, A non-fluorinated monobenzocyclooctyne for rapid copper-free click reactions, Chemistry 18 (3) (2012) 822–828.

[23] H. Pan, P. Zhang, D. Gao, Y. Zhang, P. Li, L. Liu, C. Wang, H. Wang, Y. Ma, L. Cai, Noninvasive visualization of respiratory viral infection using bioorthogonal conjugated near-infrared-emitting quantum dots, ACS Nano 8 (6) (2014) 5468–5477.

[24] H. Pan, P. Li, G. Li, W. Li, B. Hu, H. He, Z. Chen, F. Wang, L. Liu, Y. Gong, Y. Han, Y. Luo, M. Zheng, Y. Ma, L. Cai, Y. Jin, Glycometabolic bioorthogonal chemistry-guided viral transduction for robust human T cell engineering, Adv. Funct. Mater. 29 (2019) 1807528.

[25] W. Li, H. Pan, H. He, X. Meng, Q. Ren, P. Gong, X. Jiang, Z. Liang, L. Liu, M. Zheng, X. Shao, Y. Ma, L. Cai, Bio-orthogonal T cell targeting strategy for robustly enhancing cytotoxicity against tumor cells, Small 15 (4) (2019) e1804383.

[26] Y. Han, H. Pan, W. Li, Z. Chen, A. Ma, T. Yin, R. Liang, F. Chen, Y. Ma, Y. Jin, M. Zheng, B. Li, L. Cai, T cell membrane mimicking nanoparticles with bioorthogonal targeting and immune recognition for enhanced photothermal therapy, Adv. Sci. (Weinh) 6 (15) (2019) 1900251.

[27] D.T. Rodgers, M. Mazagova, E.N. Hampton, Y. Cao, N.S. Ramadoss, I.R. Hardy, A. Schulman, J. Du, F. Wang, O. Singer, J. Ma, V. Nunez, J. Shen, A.K. Woods, T.M. Wright, P.G. Schultz, C.H. Kim, T.S. Young, Switch-mediated activation and retargeting of CAR-T cells for B-cell malignancies, Proc. Natl. Acad. Sci. U. S. A. 113 (4) (2016) E459–E468.

[28] E.J. Orlando, X. Han, C. Tribouley, P.A. Wood, R.J. Leary, M. Riester, J.E. Levine, M. Qayed, S.A. Grupp, M. Boyer, B. De Moerloose, E.R. Nemecek, H. Bittencourt, H. Hiramatsu, J. Buechner, S.M. Davies, M.R. Verneris, K. Nguyen, J.L. Brogdon, H. Bitter, M. Morrissey, P. Pierog, S. Pantano, J.A. Engelman, W. Winckler, Genetic mechanisms of target antigen loss in CAR19 therapy of acute lymphoblastic leukemia, Nat. Med. 24 (10) (2018) 1504–1506.

[29] S.R. Walsh, B. Simovic, L. Chen, D. Bastin, A. Nguyen, K. Stephenson, T.S. Mandur, J.L. Bramson, B.D. Lichty, Y. Wan, Endogenous T cells prevent tumor immune escape following adoptive T cell therapy, J. Clin. Invest. 129 (2019) 5400–5410.

[30] I. Algarra, A. Garcia-Lora, T. Cabrera, F. Ruiz-Cabello, F. Garrido, The selection of tumor variants with altered expression of classical and nonclassical MHC class I molecules: implications for tumor immune escape, Cancer Immunol. Immunother. 53 (10) (2004) 904–910.

[31] E. Decaup, C. Jean, C. Laurent, P. Gravelle, S. Fruchon, F. Capilla, A. Marrot, T. Al Saati, F.X. Frenois, G. Laurent, C. Klein, N. Varoqueaux, A. Savina, J.J. Fournie, C. Bezombes, Anti-tumor activity of obinutuzumab and rituximab in a follicular lymphoma 3D model, Blood Canc. J. 3 (2013) e131.

[32] D. Zboralski, K. Hoehlig, D. Eulberg, A. Fromming, A. Vater, Increasing tumor-infiltrating T cells through inhibition of CXCL12 with NOX-A12 synergizes with PD-1 blockade, Cancer Immunol. Res. 5 (11) (2017) 950–956.

[33] H. Dai, Y. Wang, X. Lu, W. Han, Chimeric antigen receptors modified T-cells for cancer therapy, J. Natl. Cancer Inst. 108 (7) (2016) djv439.

[34] B.L. Levine, J. Miskin, K. Wonnacott, C. Keir, Global manufacturing of CAR T cell therapy, Mol. Ther. Methods Clin. Dev. 4 (2017) 92–101.

[35] M.M. D'Aloia, I.G. Zizzari, B. Sacchetti, L. Pierelli, M. Alimandi, CAR-T cells: the long and winding road to solid tumors, Cell Death Dis. 9 (3) (2018) 282.

[36] E. Lanitis, D. Dangaj, M. Irving, G. Coukos, Mechanisms regulating T-cell infiltration and activity in solid tumors, Ann. Oncol. 28 (suppl_12) (2017) xii18–xii32.

[37] C.S. Jansen, N. Prokhnevska, V.A. Master, M.G. Sanda, J.W. Carlisle, M.A. Bilen, M. Cardenas, S. Wilkinson, R. Lake, A.G. Sowalsky, R.M. Valanparambil, W.H. Hudson, D. McGuire, K. Melnick, A.I. Khan, K. Kim, Y.M. Chang, A. Kim, C.P. Filson, M. Alemozaffar, A.O. Osunkoya, P. Mullane, C. Ellis, R. Akondy, S.J. Im, A.O. Kamphorst, A. Reyes, Y. Liu, H. Kissick, An intra-tumoral niche maintains and differentiates stem-like CD8 T cells, Nature 576 (2019) 465–470.

[38] J. Zhang, S. Endres, S. Kobold, Enhancing tumor T cell infiltration to enable cancer immunotherapy, Immunotherapy 11 (3) (2019) 201–213.

[39] C. Oelkrug, J.M. Ramage, Enhancement of T cell recruitment and infiltration into tumours, Clin. Exp. Immunol. 178 (1) (2014) 1–8.

[40] K. Adachi, Y. Kano, T. Nagai, N. Okuyama, Y. Sakoda, K. Tamada, IL-7 and CCL19 expression in CAR-T cells improves immune cell infiltration and CAR-T cell survival in the tumor, Nat. Biotechnol. 36 (4) (2018) 346–351.

[41] B. Guo, M. Chen, Q. Han, F. Hui, H. Dai, W. Zhang, Y. Zhang, Y. Wang, H. Zhu, W. Han, CD138-directed adoptive immunotherapy of chimeric antigen receptor (CAR)-modified T cells for multiple myeloma, J. Cell. Immunother. 2 (1) (2016) 28–35.

[42] M. Sharpe, N. Mount, Genetically modified T cells in cancer therapy: opportunities and challenges, Dis, Model Mech 8 (4) (2015) 337–350.

[43] M.H. Kershaw, J.A. Westwood, P.K. Darcy, Gene-engineered T cells for cancer therapy, Nat. Rev. Canc. 13 (8) (2013) 525–541.